The stability of anthophyllite in the presence of quartz

JOSEPH V. CHERNOSKY, JR. AND LAURIE KNAPP AUTIO[1]

Department of Geological Sciences
University of Maine at Orono
Orono, Maine 04473

Abstract

The dehydration reactions anthophyllite = enstatite + quartz + fluid (1) and talc = anthophyllite + quartz + fluid (2) have been bracketed, with reversed experiments and PH_2O = Ptotal. Smooth curves drawn through the bracketing data for reactions (1) and (2) pass through the coordinates 2 kbar, 770°; 1.5 kbar, 755°; 1 kbar, 730°; 0.5 kbar, 680° and 3 kbar, 738°; 2 kbar, 711°; 1.5 kbar, 697°; 1 kbar, 678°; 0.5 kbar, 655°C, respectively. Synthetic quartz, anthophyllite, enstatite, and talc were used as starting materials. Reversibility was established by determining the relative growth or diminution (as judged by examining relative intensities of X-ray reflections) of the high- with respect to the low-temperature assemblages. Both curves are consistent with the solubility data of Hemley *et al.* (1977b) at 1 kbar but are not entirely compatible with the hydrothermal data of Greenwood (1963). Our experimental data indicate that the phase boundaries for reactions (1) and (2) intersect the phase boundary for the reaction (3) talc = 3 enstatite + quartz + H_2O at low pressure (below 200 bars) and are, therefore, more consistent with the anthophyllite phase diagram proposed by Hemley *et al.* than with the diagram proposed by Greenwood.

Gibbs energy difference functions calculated using bracketing data for reactions (1), (2), and (4) talc + forsterite = 5 enstatite + H_2O permit simultaneous evaluation of the free energies of formation of talc (-5513.69 ± 4.69 kJ mol^{-1}), enstatite (-1456.38 ± 1.93 kJ mol^{-1}), and anthophyllite ($-11,323.26 \pm 5.35$ kJ mol^{-1}) from the elements at 298K and 1 bar.

Introduction

Pure Mg-anthophyllite was first synthesized by Bowen and Tuttle (1949, p. 450), who concluded that "anthophyllite has no stable range of existence in the presence of water vapor." Using several combinations of natural and synthetic starting materials, Fyfe (1962) demonstrated that anthophyllite has a true stability field in the presence of excess water. Greenwood (1963) reversed four reactions involving Mg-anthophyllite and proposed a phase diagram which contained a stability field for anthophyllite. The stability field was depicted as a relatively narrow band 85°C wide which extended from low pressure to PH_2O = 20 kbar. Greenwood (1971) later recalculated the slope of the vapor conservative reaction (5) A = T + 4E (see Table 1 for symbols and notations), showed that it was much steeper than previously

reported, and modified the topology of the phase diagram he proposed in 1963. Greenwood's revised topology (Fig. 1) contained both possible enantiomorphic forms of the anthophyllite phase diagram, although he preferred the high-pressure portion.

Chernosky (1976) reversed the reactions (3) T = 3E + Q + H_2O and (4) T + F = 5E + H_2O at water pressures below 4 kbar and found that: (1) the reactions T = 3E + Q + H_2O and A = 7E + Q + H_2O intersect at the [F] invariant point near PH_2O = 5 kbar rather than at 20 kbar, provided that Greenwood's preferred slope for the anthophyllite-bearing reaction is taken at face value, and (2) the slopes for the reactions T + F = 5E + H_2O and (6) 9T + 4F = 5A + 4H_2O are inconsistent if Greenwood's preferred topology is correct.

On the basis of mineral–aqueous-solution equilibria performed at PH_2O = 1 kbar, Hemley *et al.* (1977b) suggest that the low-pressure portion of the phase diagram (Fig. 1), which shows the stability field of anthophyllite expanding with increasing tem-

perature and pressure, is correct. Hemley *et al.* located the [Q] and [F] invariant points near 500 and 200 bars PH_2O respectively.

Because anthophyllite is a potential indicator of pressure and temperature in some metamorphic rocks, we decided to reinvestigate the phase relations about the [F] invariant point. The reactions (1) A = 7E + Q + H_2O and (2) 7T = 3A + 4Q + 4H_2O were reversed between 500 and 3000 bars PH_2O in order to determine the correct topology for the anthophyllite phase diagram. Tight brackets for these two reactions in *P–T* space permit refinement of the free energies of talc, enstatite, and anthophyllite calculated from phase-equilibrium data by Zen and Chernosky (1976). Data upon which this paper is based have been presented orally (Chernosky and Knapp, 1977).

Experimental methods

Starting material

Mixtures with bulk compositions corresponding to $MgO \cdot SiO_2$ and $3MgO \cdot 4SiO_2$ were made by drying, weighing, and mixing requisite proportions of MgO (Fisher, lot 787699) and SiO_2 glass (Corning lump cullet 7940, lot 62221). MgO and SiO_2 glass were fired at 1000°C for three hours to drive off adsorbed water. Enstatite and talc were synthesized directly from the mixes whereas anthophyllite was synthesized using the "talc" mix. Examination of the synthetic products with a petrographic microscope and by X-ray diffraction revealed them to be entirely crystalline.

Starting materials used to reverse each reaction were prepared by mixing synthetic talc, enstatite, anthophyllite, and quartz in the appropriate proportions and grinding by hand for one-half hour to ensure homogeneity. The high-temperature assemblage constituted 50 weight percent (excluding H_2O) of the starting material for both reactions. The dried solid phases were combined with excess distilled deionized H_2O and sealed in 1.25cm-long gold capsules.

Procedure

All experiments were performed in horizontally-mounted, cold-seal hydrothermal vessels (Tuttle, 1949). Pressures were measured with factory-calibrated, sixteen-inch Heise gauges assumed accurate to ±0.1 percent of full scale (0–7000 and 0–4000 bars). Because the Heise gauges were used as "primary" standards, they were generally kept at room pressure, as suggested by the manufacturer; smaller diameter, less accurate gauges were used for continu-

Table 1. Symbols and notations

A	anthophyllite, $Mg_7Si_8O_{22}(OH)_2$
F	forsterite, Mg_2SiO_4
E	orthoenstatite, $MgSiO_3$
T	talc, $Mg_3Si_4O_{10}(OH)_2$
Q	quartz, SiO_2
G_f^o	standard Gibbs free energy of formation (298.15 K, 1 bar) of a phase from the elements, in J mol^{-1}
ΔG_r^o	Gibbs free energy of reaction at 1 bar and 298.15 K
G^*	Gibbs free energy of H_2O at Te and Pe according to Burnham et al.'s (1969) data, consistent with the standard state of 298.15 K and 1 bar
S_f^o	standard entropy of formation (298.15 K, 1 bar) of a phase from the elements, in J mol^{-1} deg^{-1}
$\Delta S_{f,s}$	change of the entropy of formation of the solid phases for a given reaction
V	volume
ΔV_s	volume change of the solid phases for a given reaction
Te, Pe	the temperature and pressure at which an univariant reaction is at equilibrium
1 thermochemical calorie ≈ 4.1840 joules	

ous monitoring of "line" pressures. In order to conserve valve stems and packings, pressures were not monitored daily. Rather, pressures were carefully monitored at the beginning of an experiment to guard against pressure leaks; once it was determined that a vessel was leak-free, it was isolated for periods of up to a month between pressure checks. Small pressure
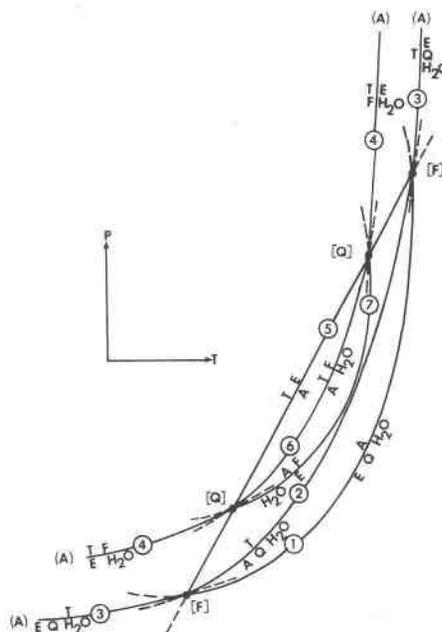
Fig. 1. Schematic *P–T* diagram after Greenwood (1971), showing the high- and low-pressure intersections of the vapor-conservative reaction A = T + 4E with the [Q] and [F] invariant points. Reactions are numbered as in the text.

fluctuations due to temperature drift were unavoidable, but experiments which experienced pressure drops of greater than 50 bars were discarded. Pressures are believed accurate to ±1 percent of the stated value.

Because temperature drifted during the experiments, daily temperature readings were averaged and the standard deviation of the temperature readings calculated; temperature errors are reported as ±2 standard deviations about the mean and represent error due to temperature drift alone. Two other sources of error in temperature must be considered; namely, errors due to a temperature gradient along a capsule and those due to inaccurate thermocouples. Temperature gradients in the pressure vessels used were all less than 1°C over a working distance of 3.0 cm (temperature calibration performed at room pressure). Because bracketing experiments were performed in 1.25cm-long sealed gold capsules, error due to temperature gradients in the pressure vessels is assumed negligible. The temperature calibration for each shielded thermocouple was checked after each experiment by heating the vessel to the temperature of the experiment at a pressure of 1 bar and comparing the measured temperature to that of a previously standardized thermocouple placed inside the bomb. This procedure insures internal consistency in temperature readings among pressure vessels, corrects for the temperature difference between the charge capsule and external measuring thermocouple, and results in an accurate temperature for an

experiment, assuming that the standard thermocouple was adequately calibrated. Corrections were usually on the order of 0–5°C. Experiments were checked for leaks both before and after hydrothermal treatment by heating the charge capsules and checking for loss of H_2O. Because quartz was generally leached from experiments which leaked, such experiments were discarded.

The products of each experiment were examined with a petrographic microscope and by X-ray powder diffraction. Because reaction rates at temperatures near the equilibrium curves were sluggish, complete reaction was generally not obtained. Judgment as to which assemblage is stable at a given pressure and temperature was based on an examination of all major reflections for the phases of interest on a diffractometer trace over the interval 5° to 40° 2θ (CuKα radiation). A reaction was considered reversed if a 25 percent change in the intensities of X-ray reflections relative to those of the starting material could be observed after the completion of an experiment. Microscopic observation of the experimental products revealed distinct textural features (described in detail later) which indicated reaction direction. Unfortunately, the sensitivity obtained using textural features to judge reaction direction was not significantly greater than the sensitivity afforded by the X-ray technique. Consequently, textural features were used to confirm the X-ray results but were not used as the sole criteria for judging reaction direction.

Unit-cell parameters for synthetic phases used in the starting material were calculated by refining power patterns obtained using an Enraf-Nonius FR552 Guinier camera and CuKα radiation; CaF_2 (Baker Lot 91548, $a = 5.4620±0.0005$A), standardized against gem diamond ($a = 3.56703$A, Robie et al., 1967), was used as an internal standard. Least-squares unit-cell refinements were performed with a computer program written by Appleman and Evans (1973).

Results

Synthesis and characterization of phases

Enstatite ($MgSiO_3$) was synthesized hydrothermally at 815°C and $PH_2O = 1$ kbar in five to seven days from a mixture of MgO and SiO_2 glass. Crystals were fine-grained (10μ), prismatic, and had parallel extinction. The X-ray pattern and unit-cell parameters (Table 2) compare favorably to the powder pattern of orthorhombic enstatite from the Bishopville meteorite (ASTM powder pattern 7-216).

Table 2. Unit-cell parameters and volumes of synthetic enstatite, talc, and anthophyllite

	enstatite	talc	anthophyllite
a	18.236(10)	5.291(6)	18.57(4)
b	8.822(3)	9.169(7)	17.91(4)
c	5.176(1)	18.982(16)	5.25(1)
V	832.86 (43)	909.47 (1.28)	1748.0 (3.7)
β	----	99°4'	----
N	19	14	16
S	CaF$_2$	CaF$_2$	CaF$_2$

Figures in parentheses represent the estimated standard deviation in terms of least units cited for the value to their immediate left; these uncertainties were calculated using the cell refinement program and represent precision only. Cell parameters are expressed in angstroms.

Abbreviations: N = number of reflections used in unit cell refinement; S = X-ray standard.

Talc [$Mg_3Si_4O_{10}(OH)_2$] was synthesized hydrothermally at 680°C, PH_2O = 2 kbar in five to ten days. The synthetic product typically crystallized as aggregates of very fine-grained plates and contained less than 0.5 percent forsterite as an impurity, which could be due to leaching of silica from the starting material or to the initial preparation of a starting material deficient in SiO_2. The powder pattern and unit-cell parameters of talc (Table 2) compare favorably with those of natural (ASTM powder pattern 13-558) and synthetic (Forbes, 1971) talc.

Anthophyllite [$Mg_7Si_8O_{22}(OH)_2$] was synthesized together with cristobalite, enstatite, talc, forsterite, and quartz by hydrothermally treating synthetic talc at 840°C, PH_2O = 0.5 kbar for 12 hours. A mixture of anthophyllite and quartz together with about 5 percent talc was obtained by hydrothermally treating the products of the previous experiment at 735°C, PH_2O = 3 kbar for 41 days. Anthophyllite synthesized in this manner occurred as extremely fine grains intimately intergrown with talc, and as somewhat larger (10µ) prismatic crystals having parallel extinction. The X-ray powder pattern and unit-cell parameters (refined assuming the anthophyllite space group *Pnma*) correspond favorably to those of synthetic (Greenwood, 1963) and natural (Finger, 1970) anthophyllite. Because several new triple-chain minerals created during the reaction of anthophyllite to form talc have recently been reported (Veblen and Burnham, 1975, 1976; Veblen *et al.*, 1977), we compared the powder patterns of synthetic anthophyllite to calculated powder patterns of jimthompsonite, clinojimthompsonite, and chesterite provided by D. R. Veblen. Reflections belonging to these phases were not observed in the synthetic anthophyllite we used as starting material. D. R. Veblen kindly examined the starting material and the products of several reversal experiments on both sides of each phase boundary with a high-resolution transmission electron microscope and observed isolated slabs of a triple-chain silicate parallel to 010 of anthophyllite. The percentage of triple-chain silicate varied (5–15 percent by volume) from one grain to the next. The triple-chain silicate apparently forms when anthophyllite is initially synthesized outside its stability field from talc. X-ray reflections from the triple-chain silicate were not observed because the isolated slabs are only one unit cell thick.

We assume that the presence of triple-chain impurities does not significantly affect the experimental results, because the ratio of anthophyllite to triple-chain silicate is the same after the completion of a bracketing experiment as it is in the starting material. Interaction of triple-chain impurities with the fluid phase is probably minimized because dissolution of anthophyllite during a bracketing experiment presumably occurs along grain boundaries, and the triple-chain impurities are located within anthophyllite grains.

Quartz (SiO_2) was synthesized together with anthophyllite with synthetic talc as a starting material. The positions of the major X-ray reflections of the synthetic quartz compare favorably to those of natural quartz from Lake Toxaway, North Carolina (ASTM powder pattern 5-0490); unfortunately, the number of reflections required for a unit-cell refinement was not observed in the synthetic product, which contained less than 11 percent quartz.

The reaction A = 7E + Q + H₂O

Starting material used for reversing reaction (1), A = 7E + Q + H_2O, was obtained by mixing pure synthetic enstatite together with anthophyllite and quartz. The starting material contained a small amount (<5 percent) of talc which, however, reacted away in all but three experiments (Table 3, Experiments 5, 21, and 24) located near the metastable extension of the phase boundary for reaction (3), T = 7E + Q + H_2O. Petrographic examination of experimental products which showed definite reaction revealed that the dimensions of crystals belonging to

Table 3. Experiments bracketing the reaction A = 7E + Q + H₂O

Experiment number	T (°C)	P_{H_2O} (kbars)	Duration (hours	Comments	
24	664(1.5)	0.5	837	A(+)E(-)Q(-)T(+)	M
23	687(2)	0.5	2607	A(-)E(+)Q(+)	S
11	758(3)	0.5	1080	A(-)E(+)Q(+)	W
22	699.5(1.5)	1.0	816	A(+)E(-)Q(-)	M
21	719.5(3.5)	1.0	936	A(+)E(-)Q(-)T(+)	M
19	760(1)	1.0	974	A(-)E(+)Q(+)	S
12	737(1.5)	1.5	1273	A(+)E(-)Q(-)	W
13	752(2)	1.5	1224	A(+)E(-)Q(-)	W
14	767(4)	1.5	1105	A(-)E(+)Q(+)	M
6	733(2)	2.0	1080	A(+)E(-)Q(-)	M
9	751(1.5)	2.0	630	A(+)E(-)Q(-)	M
5	765(3.5)	2.0	744	A(+)E(-)Q(-)T(+)	M
25	775(2)	2.0	857	A(-)E(+)Q(+)	M
20	754.5(2.0)	3.0	818	A(+)E(-)Q(-)	M

Growth or diminution of a phase is indicated by a (+) or (-) respectively. All assemblages include vapor. Parenthesized numbers represent two standard deviations in terms of least units cited for the mean temperatures to their immediate left. Symbols S, M, and W are qualitative estimates of the extent of reaction and represent greater than 80 percent, 80 to 50 percent, and less than 50 percent reaction, respectively.

the stable assemblage increased, whereas crystals belonging to the unstable assemblage had corroded grain boundaries. Several additional textural features were observed in experiments conducted on the high-temperature side of the phase boundary: (1) quartz often recrystallized to the point where undulatory extinction became evident, (2) fine quartz grains (2μ) occurred as inclusions oriented parallel to the c axis of enstatite, and (3) very fine (0.5μ) quartz grains were observed to cluster about the periphery of larger enstatite crystals, suggesting that a single anthophyllite grain had reacted to enstatite + quartz.

Critical experiments used to bracket the position of the univariant curve for reaction (1) are set down in Table 3 and are plotted on Figure 2, where they are compared to results of other workers who have used both synthetic and natural anthophyllite as starting material. The smooth curve through the experimental brackets was constructed using a log $f\mathrm{H_2O} - 1/T$ diagram. Although our experimental data are consistent with all but one ($P\mathrm{H_2O} = 2.6$ kbar, 775°C) reversal obtained by Greenwood (1963), the slope of the curve drawn through our data is shallower than the curve (Fig. 2, dashed line) suggested by him. Greenwood also converted natural anthophyllite containing 11.12 percent FeO to enstatite + quartz, but did not attempt to convert enstatite + quartz to Fe-bearing anthophyllite. Fyfe (1962) obtained three reversals at $P\mathrm{H_2O} = 2$ kbar (Fig. 2), using a fairly

Fig. 2. Dehydration curve for the reaction A = 7E + Q + H₂O. Solid symbols represent growth of anthophyllite; open symbols represent growth of the high-temperature assemblage. Size of rectangles represents uncertainty in measurement of pressure and temperature. Dashed curve is after Greenwood (1963).

pure natural anthophyllite (2.77 percent MnO, 1.26 percent CaO, and 0.59 percent $\mathrm{Al_2O_3}$) from Falconville, New York. The phase boundary determined in this study passes through an equilibrium point at 729°C, $P\mathrm{H_2O} = 1$ kbar calculated by Hemley *et al.* (1977b), using thermochemical values derived from their experimental data on several reactions in the system $\mathrm{MgO-SiO_2-H_2O}$.

The reaction 7T = 3A + 4Q + 4H₂O

The starting material used for reversing reaction (2), 7T = 3A + 4Q + 4H₂O, consisted of an intimately intergrown mixture of fine-grained talc (50 percent), anthophyllite (44.7 percent), and quartz (5.3 percent), all synthesized simultaneously from a mix having the composition of talc. The starting material also contained a small amount (<0.5 percent) of a fine (30μ), colorless, isotropic impurity having conchoidal fracture and $n_\mathrm{D} \approx 1.58$. The amount of this impurity decreased substantially during the bracketing experiments.

Although textural relations alone did not provide unambiguous criteria for determining reaction direction, several textural features confirmed X-ray results. An experiment conducted within the stability field of the high-temperature assemblage generally contained many well-shaped anthophyllite needles and recrystallized quartz grains having undulatory extinction. On the other hand, experiments conducted within the stability field of the low-temperature assemblage contained very fine, barely distinguishable quartz grains and occasional euhedral talc plates rather than anthophyllite needles.

Critical experiments which bracket the position of the univariant curve for reaction (2) are set down in Table 4 and plotted on Figure 3. The smooth curve through the experimental brackets was constructed using a log $f\mathrm{H_2O} - 1/T$ diagram. Our experimental data are not entirely consistent with the reversals obtained by Greenwood (1963). Although our phase boundary passes through Greenwood's bracket at $P\mathrm{H_2O} = 2$ kbar, it has a shallower slope than Greenwood's proposed phase boundary (Fig. 3, dashed line). Our curve passes through an equilibrium point at 675°±7°C, $P\mathrm{H_2O} = 1$ kbar obtained by Hemley *et al.* (1977b), who monitored phase changes of the solids and compositions of the aqueous solutions in equilibrium with these solids. They used a variety of starting materials, including natural anthophyllite containing 5.9 percent FeO or the same anthophyllite exchanged with 1M $\mathrm{MgCl_2}$ at 720° and 2 kbar.
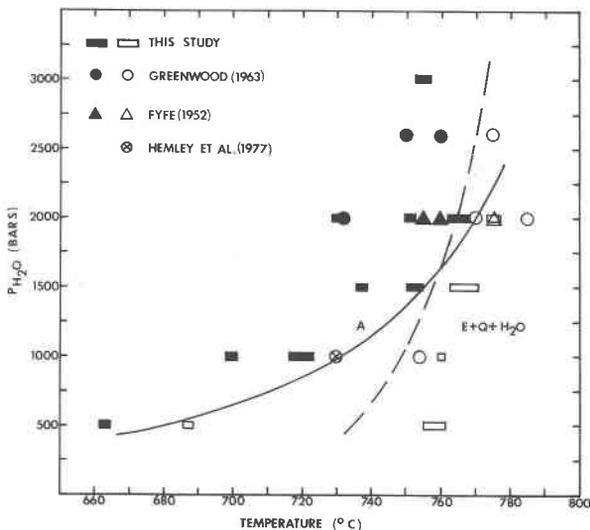
Thermochemical calculations

Zen and Chernosky (1976) calculated the free energies of talc, enstatite, and anthophyllite using phase equilibrium data of Greenwood (1963) and Chernosky (1976). Unfortunately, the uncertainties in the calculated free energies were rather large: ± 10.5 kJ mol^{-1} for talc, ± 17 kJ mol^{-1} for anthophyllite, and ± 4 kJ mol^{-1} for enstatite. The bracketing data obtained during this study have enabled us to refine the free energies of these phases and reduce the uncertainties of the calculated values.

The Gibbs free energy of formation of a phase from the elements at 298K, 1 bar can be calculated from the P–T coordinates of a phase boundary using the relation (Fisher and Zen, 1971):

$$\Delta G(Te,Pe) = 0 = \Delta G^0_{f,s}(298,1) - \int_{298}^{Te} \Delta S^0_{f,s} dT$$

$$+ \int_1^{Pe} \Delta V_s dP + G^*(H_2O)(Te,Pe)$$

The integrals $\int \Delta S^0_{f,s} dT$ and $\int \Delta V_s dP$ have been approximated by the quantities $\Delta S^0_{f,s} \Delta T$ and $\Delta V_s \Delta P$, respectively. The uncertainty introduced by making these substitutions is small (Zen, 1969).

We have chosen to calculate the free energies of talc, enstatite, and anthophyllite by simultaneously evaluating the Gibbs energy difference functions (Thompson, 1973) $G^0_f(A) - 7G^0_f(E)$, $7G^0_f(T) - 3G^0_f(A)$, and $G^0_f(T) - 5G^0_f(E)$, for the reactions A = 7E + Q + H$_2$O, 7T = 3A + 4Q + 4H$_2$O, and T + F = 5E + H$_2$O, respectively (Table 5). The uncertainty attached to the difference functions calculated for each individual experiment (Table 5) was evaluated by combining, in the commonly accepted manner, the uncertainties associated with the free energies of either quartz or forsterite, the entropies and molar volumes of the solid phases, and the values for $G^*(H_2O)$. The uncertainty attached to the average value for each difference function (Table 5) was obtained by adding the uncertainties in the primary thermochemical data (Table 6) to the uncertainties reflected in the finite width of each experimental bracket (Figs. 2 and 3). The "best" value for each difference function ($\hat{G}_i$) and its associated uncertainty ($\hat{g}_i$) were calculated using the relations:

$$\hat{G}_i = \Sigma_{i=1}^K G_i w_i / \Sigma_i w$$

and

$$\hat{g}_i = (1/\Sigma_{i=1}^K w_i)^{1/2}$$

where g_i is the uncertainty associated with G_i and $w_i \equiv 1/g_i^2$. This procedure was used by Zen (1972) and

has been lucidly explained by Bird and Anderson (1973).

In order to evaluate the difference functions, one only needs the free energies of quartz and forsterite at 298K, 1 bar, the molar volumes and entropies of the

Table 4. Experiments bracketing the reaction 7T = 3A + 4Q + 4H$_2$O

Experiment number	T (°C)	P_{H_2O} (kbars)	Duration (hours)	Comments	
15	613(3)	0.5	1061	T(+)A(-)Q(-)	M
14	630(3)	0.5	1061	T(+)A(-)Q(-)	M
10	647(3.5)	0.5	2544	T(+)A(-)Q(-)	W
12	677(1)	0.5	1052	T(-)A(+)Q(+)	M
8	664(1)	1.0	744	T(+)A(-)Q(-)	M
5	687(3)	1.0	872	T(-)A(+)Q(+)	M
6	714(3)	1.0	744	T(-)A(+)Q(+)	M
19	693(3)	1.5	1826	T(+)A(-)Q(-)	W
9	701(3)	1.5	1399	T(-)A(+)Q(+)	M
20	706(4)	2.0	2760	T(+)A(-)Q(-)	W
17	719(2)	2.0	1014	T(-)A(+)Q(+)	W
7	692(1)	3.0	799	T(+)A(-)Q(-)	S
13	720(4)	3.0	1651	T(+)A(-)Q(-)	S
21	727(4)	3.0	2688	T(+)A(-)Q(-)	W
16	742(4)	3.0	993	T(-)A(+)Q(+)	W

Growth or diminution of a phase is indicated by (+) or (-) respectively. All assemblages include vapor. Parenthesized numbers represent two standard deviations in terms of least units cited for the mean temperatures to their immediate left. Symbols S, M, and W are qualitative estimates of the extent of reaction and represent greater than 80 percent, 80 to 50 percent, and less than 50 percent reaction, respectively.

Fig. 3. Dehydration curve for the reaction 7T = 3A + 4Q + 4H$_2$O. Solid symbols represent growth of talc; open symbols represent growth of the high-temperature assemblage. Size of rectangles represents uncertainty in measurement of pressure and temperature. Dashed curve is after Greenwood (1963).

Table 5. Gibbs energy difference functions for three equilibria in the system $MgO-SiO_2-H_2O$

```
(1)   A = 7E + Q + H₂O

      G°f(A) - 7G°f(E) = G°f(Q) + G*(H₂O) + ΔVsΔP - ΔSsΔT

P,kbar      Lower temp. reversal        Upper temp. reversal

0.5         664°C  -1127.27±0.98        687°C  -1129.14±0.97
1.0         720    -1128.01±0.96        760    -1130.75±0.96
1.5         752    -1128.36±0.95        767    -1129.31±0.95
2.0         765    -1128.09±0.95        775    -1128.63±0.95

Average ± 1 standard error:        1128.59±0.79    kJ mol⁻¹

(2)   7T = 3A + 4Q + 4H₂O

      7G°f(T) - 3G°f(A) = 4G°f(Q) + 4G*(H₂O) + ΔVsΔP - ΔSsΔT

P,kbar      Lower temp. reversal        Upper temp. reversal

0.5         647    -4621.75±1.96        677    -4636.84±1.95
1.0         664    -4616.88±1.94        687    -4627.50±1.93
1.5         692    -4623.07±1.93        701    -4626.99±1.92
2.0         681    -4624.71±1.92        719    -4630.30±1.91
3.0         727    -4627.45±1.90        742    -4633.57±1.90

Average ± 1 standard error:        -4626.07±2.34    kJ mol⁻¹

(3)   T + F = 5E + H₂O

      G°f(T) - 5G°f(E) = -G°f(F) + G*(H₂O) + ΔVsΔP - ΔSsΔT

P,kbar      Lower temp. reversal        Upper temp. reversal

0.5         600    1769.92±1.10         621    1767.78±1.09
1.0         637    1768.90±1.09         657    1767.05±1.08
2.0         640    1770.38±1.08         663    1768.45±1.08
3.0         662    1769.30±1.07         692    1766.87±1.07
4.0         686    1767.79±1.07         706    1766.24±1.06

Average ± 1 standard error:        1768.21±0.92    kJ mol⁻¹
```

Bracketing data for reaction (3) is from Chernosky (1976).

solid phases (Table 6), and values for $G*(H_2O)$, the standard Gibbs free energy of water, tabulated by Fisher and Zen (1971). The heat capacities of quartz, forsterite, and talc have been measured and the entropy values derived from these measurements are probably of high quality. We assume that the entropy of clinoenstatite is a good approximation for ortho-enstatite (Zen and Chernosky, 1976, p. 1158).

A major source of uncertainty is the entropy of anthophyllite; the value used by Zen (1971) and by Zen and Chernosky (1976) was calculated by Mel'nik and Onoprienko (1969) from Greenwood's (1963) phase equilibrium data for the reaction A = 7E + Q + H_2O. Although our bracketing data for this reaction are consistent with all but one of Greenwood's reversals (Fig. 3), they more closely define the position of the equilibrium curve and hence provide a useful check on the entropy of anthophyllite.

We have used Gordon's (1973) method for obtaining the range of permissible ΔG_r^0 and $\Delta S_{f,s}^0$ values which together satisfy a set of linear inequalities of the form:

$$\Delta G_r^0 - (T-298)\Delta S_{f,s}^0 + (P-1)\Delta V_s + G*(H_2O) \gtrless 0$$

Each linear inequality of the set is obtained from an experimental reversal of the reaction A = 7E + Q + H_2O (Table 3). The range of permissible $\Delta S_{f,s}^0$ values which satisfy the inequalities is 177.7 to 201.4 J mol⁻¹ deg⁻¹ which corresponds to $S_f^0(A)$ values ranging from −2398 to −2422 J mol⁻¹ deg⁻¹, respectively. We have adopted Mel'nik and Onoprienko's entropy value (−2411 J mol⁻¹ deg⁻¹) for anthophyllite because it lies within the middle of this permissible range of values, and have assigned to it an uncertainty of ±12 J mol⁻¹ deg⁻¹.

The calculated value for $G_f^0(T) - 5G_f^0(E)$ (Table 5) is about 1 kJ smaller than the value obtained by Zen and Chernosky (1976), who replaced the integral $\int \Delta S_{f,s}^0 dT$ by $\sum \Delta \bar{S}_{f,s} \Delta T$ rather than by $\Delta S_{f,s}^0 \Delta T$; the mean value, $\Delta \bar{S}_{f,s}$, is obtained from entropy of formation values for successive even-hundred-degree intervals. We did not use the approximation made by Zen and Chernosky because $S_f^0(A)$ is not known as a function of temperature; in addition, our procedure requires that all three difference functions be calculated in the same manner. Simultaneous evaluation of the three difference functions (Table 5) yields the following: $G_f^0(A) = -11323.26\pm5.35$, $G_f^0(E) = -1456.38\pm1.93$, and $G_f^0(T) = -5513.69\pm4.69$ kJ mol⁻¹, where the errors are ±2 standard deviations. The calculated free energies are in excellent agreement with those obtained by Zen and Chernosky

Table 6. Thermodynamic parameters of phases

	$G_f^0(298,1)$ kJ mol⁻¹	$S_f^0(298,1)$ J mol⁻¹deg⁻¹	$V(298,1)$ J bar⁻¹gf⁻¹
Anthophyllite $Mg_7Si_8O_{22}(OH)_2$	−11323.26 ±5.35 (3)	−2411 ±12 (3)	26.446 (6)
Enstatite $MgSiO_3$	−1456.38 ±1.93 (3)	−291.14 ±0.46† (2)	3.1476 ±0.0050 (5)
Forsterite Mg_2SiO_4	−2051.70 ±1.9* (4)	−398.99 ±0.88 (2)	4.3786 ±0.0029 (5)
Quartz SiO_2	−856.239 ±1.72 (1)	−182.49 ±0.08 (2)	2.2689 ±0.0003 (5)
Talc $Mg_3Si_4O_{10}(OH)_2$	−5513.69 ±4.69 (3)	−1273.08 ±0.71 (2)	13.6252 ±0.0259 (5)

Number in parentheses refers to source of data: (1) Robie and Waldbaum (1968); (2) Zen (1972); (3) this study; (4) Hemingway and Robie (unpub. data); (5) Robie et al. (1967); (6) Zen (1971).

*Value corrected in accordance with the revised value for the heat of solution of quartz.

†Value refers to clinoenstatite.

(1976), but the associated uncertainties are considerably smaller.

Free-energy values for anthophyllite (-11344.17 ± 7.11), enstatite (-1460.63 ± 2.51), and talc (-5524.60 ± 3.77 kJ mol^{-1}) calculated by Hemley *et al.* (1977a) and Hemley *et al.* (1977b) differ from those obtained in this paper, despite excellent agreement among the phase equilibrium data. The discrepancy in the calculated free energies of enstatite and anthophyllite is directly related to the free energy value used for talc. Hemley *et al.* (1977a) calculated $G_f^0(T)$ from experimental data for the equilibrium

$$Mg_3Si_4O_{10}(OH)_2 + 5H_2O$$
$$= Mg_3Si_2O_5(OH)_4 + 2H_4SiO_4$$
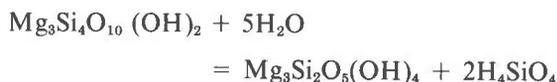
at 200°C, 100 bars; in order to perform the calculation, the free energies of H_4SiO_4 and chrysotile as well as entropies and molar volumes of talc and chrysotile and heat capacities of chrysotile, talc, H_2, O_2, and Si are required. Hemley *et al.* (1977b) used values for $G_f^0(T)$ and $G_f^0(F)$ reported by Robie and Waldbaum (1968) to calculate $G_f^0(A)$ and $G_f^0(E)$. However, the value for $G_f^0(F)$ contained in Robie and Waldbaum (1968) has been revised by Hemingway and Robie (unpublished data) due to a revision in the enthalpy of solution of α-quartz (Hemingway and Robie, 1977). Inasmuch as we used 28 experimentally-determined P-T coordinates and more recent ancillary thermochemical values, we believe our calculated free energies for talc, enstatite, and anthophyllite are more accurate.

Discussion

Cursory inspection of the phase boundaries for reactions (1), $A = 7E + Q + H_2O$, and (2), $7T = 3A + 4Q + 4H_2O$, (Figs. 2 and 3) suggests that they will intersect and generate the [F] invariant point at a water pressure below 200 bars. Additional constraint on the location of the [F] invariant point is obtained by including phase-equilibrium data (Chernosky, 1976) for reaction (3), $T = 3E + Q + H_2O$. Provided that the activities of all the phases participating in the reaction are unity and that steam is the only volatile species involved in the reaction, van't Hoff's equation reduces to:

$$(\partial \log f_{H_2O}^n)\partial 1/T)_{P_s} = -(\Delta H)_{P_s}/2.303R$$

This relation indicates that a dehydration boundary will plot as a straight line on a $\log fH_2O - 1/T$ diagram if ΔH at constant P_s is constant (Orville and Greenwood, 1965). It is necessary to correct the slope
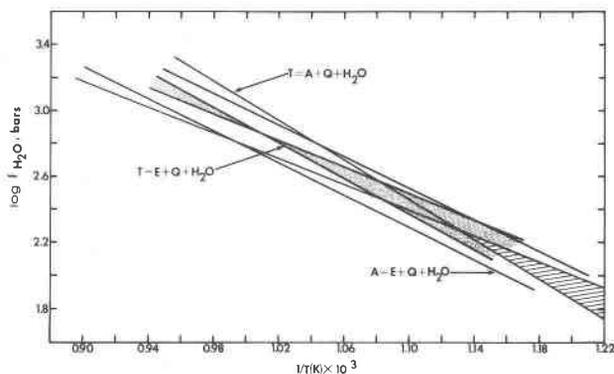
Fig. 4. Log $fH_2O - 1/T$ plot for reactions (1), (2), and (3). Experimental data for reactions (1) and (2) are taken from this study; data for reaction (3) are from Chernosky (1976). Lined area shows possible location of [F] invariant point. Limiting slopes of reactions have been plotted as they would have appeared if the experiments had all been performed at a constant total pressure of 1 bar.

of the phase boundary for the effect of pressure on volume change of the solid phases (Eugster and Wones, 1962, p. 91). The correction amounts to recalculating data for experiments at variable total pressure so that they appear as if they were obtained at the same constant total pressure, using the expression

$$\Delta \log f_{H_2O}^n = -\Delta V s(P - P\text{exp})/2.303RT$$

where P is the pressure to which the experiments are being adjusted, Pexp is the experimentally-determined pressure, and n is the number of moles of water participating in the reaction.

Phase boundaries for reactions (1), (2), and (3) have been plotted on a $\log fH_2O - 1/T$ diagram (Fig. 4); all experiments have been recalculated to a total pressure of 1 bar. Individual reversals have been omitted from Figure 4 for the sake of clarity; however, the limiting slopes for each reaction are shown. In constructing Figure 4, we have assumed that there is no solid solution between anthophyllite and the triple-chain silicate and that anthophyllite does not change composition during the course of the experiments. Figure 4 indicates that all three reactions can intersect below $PH_2O = 200$ bars, and suggests that the phase diagram proposed by Hemley *et al.* (1977b), who placed the [F] invariant point at 200 bars, is consistent with the data presented in this paper. However, because the reactions intersect at a low angle, we cannot locate [F] precisely nor can we rule out the possibility of a high-pressure intersection. In fact, Evans (1977) has suggested that both

the high- and low-pressure portions of the phase diagram as depicted in Figure 1 may exist.

Thus far, we have considered the triple-chain (TC) silicate an impurity and have assumed that it does not affect the location of the phase boundaries. The chief reason for assuming no solid solution between the TC silicate and anthophyllite is that the structures of these two phases are different. We know, however, that the TC silicate is not inert, since the ratio of TC silicate to anthophyllite remains nearly constant during the reversal experiments, even though anthophyllite either grows or decomposes. It is difficult to quantitatively evaluate the effect of the TC silicate because its thermochemical parameters and its relationship to the host anthophyllite are unknown.

One way to obtain quantitative information on the effect of the TC silicate in anthophyllite is to consider that there is solid solution between the two phases. Strictly speaking this approximation is incorrect. However, it is reasonable because (1) the structures of the two phases are very similar, and (2) the randomly-distributed domains of the TC silicate in anthophyllite are on the order of one unit cell thick. Although Veblen observed that the amount of TC silicate varied (5 to 15 percent) from one anthophyllite grain to the next, the average was about 10 percent. Assuming the presence of 10 percent jimthompsonite, $Mg_{10}Si_{12}O_{32}(OH)_4$, in anthophyllite, the formula for the anthophyllite–jimthompsonite solid solution ($A_{90}JT_{10}$) becomes $Mg_{7.3}Si_{8.4}O_{23}(OH)_{2.2}$. When recast to preserve stoichiometry, reactions (1) and (2) become:

$$10A_{90}JT_{10} = 73E + 11Q + 11H_2O \qquad (1a)$$

and

$$73T = 30A_{90}JT_{10} + 40Q + 40H_2O \qquad (2a)$$

In order to evaluate the free energy of $A_{90}JT_{10}$, we need its molar volume and entropy. Although these quantities are not known, the molar volume of the "solid solution" should be close to the molar volume of anthophyllite. The error introduced by using the molar volume of the synthetic anthophyllite (Table 2) used in the starting material is negligible. We have also assumed that the entropy contribution of the TC "impurity" is within the limits (-2411 ± 12 J mol^{-1} deg^{-1}) calculated using experimental data for the reaction $A = 7E + Q + H_2O$. Although this assumption is highly suspect because configuration and mixing contributions to the entropy have been ignored, the error introduced is probably far smaller than the error arising from the uncertainties in the free energies of the other phases involved in the reactions.

Using the approximations mentioned above, Gibbs energy difference functions, $10\ G_f^0(A_{90}JT_{10}) - 73\ G_f^0(E)$ and $73\ G_f^0(T) - 30\ G_f^0(A_{90}JT_{10})$, were calculated. These values were combined with those for $G_f^0(T) - 5\ G_f^0(E)$ (Table 5) and solved simultaneously to yield: $G_f^0(T) = -5514.00\pm12.78$, $G_f^0(E) = -1456.44\pm2.83$, and $G_f^0(A_{90}JT_{10}) = -11,785.67\pm15.66$ kJ mol^{-1}.

Although the calculated free energy of $A_{90}JT_{10}$ is tentative, it suggests that the addition of the component $Mg_{10}Si_{12}O_{32}(OH)_4$ stabilizes pure Mg-anthophyllite. The amount by which pure Mg-anthophyllite is stabilized will undoubtedly change as more accurate values for the molar volumes and entropies of the A–JT solid solutions become available; however, it is unlikely that the direction of change, at least for Mg-rich compositions, will be affected, i.e., our calculated free energy for pure Mg-anthophyllite is probably a "least stable" value.

Because our experimental work was conducted using Fe-free phases as starting materials with water pressure essentially equal to total pressure, it necessarily has limited direct application to natural rocks. The effects of decreasing PH_2O relative to Pfluid or to Ptotal are well known (Thompson, 1955; Greenwood, 1961) and will not be discussed. The effect of substituting Fe^{2+} for Mg on the phase boundaries considered in this paper is a topic of current debate.

Calculations by Evans and Trommsdorff (1974) assuming $X_{Mg}(E) = 0.900$, $X_{Mg}(T) = 0.973\pm0.002$, and $X_{Mg}(A) = 0.88\pm0.01$ suggest that the equilibrium $A = T + 4E$ will occur at a lower pressure or a higher temperature in the iron-free system by an amount given by $\Delta T = RT/\Delta S \ \ln K \simeq 200\pm95°C$. Evans (1977) calculated that the temperature shift due to the substitution of 10 mole percent Fe for Mg in the other anthophyllite-bearing reactions should be small ($\sim\pm10°C$), because the volume and entropy changes are much greater for dehydration reactions than for vapor-conservative reactions. However, Sanford (1977) using different values for the enthalpies of formation of the phases involved, calculated that the substitution of Fe^{2+} for Mg by an amount commonly observed in natural occurrences is sufficient to lower the phase boundary for the reaction $9T + 4F = 5A + 4H_2O$ by $120°–150°C$, assuming $PH_2O = P$total.

Sanford's result is surprising in light of experimental data for the reaction $7T = 3A + 4Q + 4H_2O$, obtained by Hemley et al. (1977b) using as starting materials both natural anthophyllite containing 5.9 percent FeO and the same anthophyllite in which the iron had been exchanged for Mg. Hemley et al. (1977b, p. 362) stated that "No systematic differences

were noted in the use of natural *vs.* synthetic or exchanged *vs.* unexchanged materials." Clearly, additional experimental work on the stability of Fe-bearing anthophyllite will be extremely useful in resolving this problem.

References

Appleman, D. E. and H. T. Evans, Jr. (1973) Job 9214: Indexing and least squares refinement of powder diffraction data. *Natl. Tech. Inf. Serv., U.S. Dept. Commerce, Springfield, Virginia, Document PB-216 188.*

Bird, G. W. and G. M. Anderson (1973) The free energy of formation of magnesian cordierite and phlogopite. *Am. J. Sci., 273,* 84–91.

Bowen, N. L. and O. F. Tuttle (1949) The system MgO–SiO₂–H₂O. *Geol. Soc. Am. Bull., 60,* 439–460.

Burnham, C. W., J. R. Hollaway and N. F. Davis (1969) Thermodynamic properties of water to 1000°C and 10,000 bars. *Geol. Soc. Am. Spec. Pap. 132.*

Chernosky, J. V., Jr. (1976) The stability field of anthophyllite—A reevaluation based on new experimental data. *Am. Mineral., 61,* 1145–1155.

—— and L. A. Knapp (1977) The stability of anthophyllite plus quartz. *Geol. Soc. Am. Abstracts with Programs, 9,* 927.

Eugster, H. P. and D. R. Wones (1962) Stability relations of the ferruginous biotite, annite. *J. Petrol., 3,* 82–125.

Evans, B. W. (1977) Metamorphism of Alpine peridotite and serpentinite. *Ann. Rev. Earth Planet. Sci., 5,* 397–447.

—— and V. Trommsdorff (1974) Stability of enstatite + talc, and CO₂-metasomatism of metaperidotite, Val d'Efra, Lepontine Alps. *Am. J. Sci., 274,* 274–296.

Finger, L. W. (1970) Refinement of the crystal structure of anthophyllite. *Carnegie Inst. Wash. Year Book, 68,* 283–288.

Fisher, J. R. and E-an Zen (1971) Thermodynamic calculations from hydrothermal phase equilibrium data and the free energy of H₂O. *Am. J. Sci., 270,* 297–314.

Forbes, W. C. (1971) Iron content of talc in the system Mg₃Si₄O₁₀(OH)₂–Fe₃Si₄O₁₀(OH)₂. *J. Geol., 79,* 63–74.

Fyfe, W. S. (1962) On the relative stabilities of talc, anthophyllite and enstatite. *Am. J. Sci., 270,* 151–154.

Gordon, T. M. (1973) Determination of internally consistent thermodynamic data from phase equilibrium experiments. *J. Geol., 81,* 199–208.

Greenwood, H. J. (1961) The system NaAlSi₂O₆–H₂O–argon: total pressure and water pressure in metamorphism. *J. Geophys. Res., 66,* 3923–3946.

—— (1963) The synthesis and stability field of anthophyllite. *J. Petrol., 4,* 317–351.

—— (1971) Anthophyllite. Corrections and comments on its stability. *Am. J. Sci., 270,* 151–154.

Hemingway, B. S. and R. A. Robie (1977) Enthalpies of formation of low albite (NaAlSi₃O₈), gibbsite (Al(OH)₃), and NaAlO₂;

revised values for ΔH°$_{f,298}$ and ΔG°$_{f,298}$ of some aluminosilicate minerals. *J. Res. U.S. Geol. Surv., 5,* 413–429.

Hemley, J. J., J. W. Montoya, C. L. Christ and P. B. Hostetler (1977a) Mineral equilibria in the MgO–SiO₂–H₂O system: I. Talc–chrysotile–forsterite–brucite stability relations. *Am. J. Sci., 277,* 351.

——, ——, D. R. Shaw and R. W. Luce (1977b) Mineral equilibria in the MgO–SiO₂–H₂O system: 11 Talc–antigorite–forsterite–anthophyllite–enstatite stability relations and some geologic implications in the system. *Am. J. Sci., 277,* 353–383.

Mel'nik, Yu. P. and V. L. Onoprienko (1969) Termodinamicheskiye svoystva antofillita. In *Konstitutsiya i Svoystva Mineralov,* Vol. 3 (Thermodynamic properties of anthophyllite, In *Constitution and Properties of Minerals,* Vol. 3), p. 46–55. Akad. Nauk Ukr. SSR, Kiev.

Orville, P. M. and H. J. Greenwood (1965) Determination of ΔH of reaction from experimental pressure–temperature curves. *Am. J. Sci., 263,* 678–683.

Robie, R. A., P. M. Bethke and K. M. Beardsley (1967) Selected X-ray crystallographic data, molar volumes, and densities of minerals and related substances. *U.S. Geol. Surv. Bull. 1248.*

—— and D. R. Waldbaum (1968) Thermodynamic properties of minerals and related substances at 298.15°K (25.0°C) and one atmosphere (1.013 bars) pressure and at higher temperatures. *U.S. Geol. Surv. Bull. 1259.*

Sanford, R. F. (1977) The coexistence of antigorite and anthophyllite in ultramafic rocks (abstr.). *Geol. Soc. Am. Abstracts with Programs, 9,* 1154–1155.

Thompson, A. B. (1973) Analcime: free energy from hydrothermal data. Implications for phase equilibria and thermodynamic quantities for phases in NaAlO₂–SiO₂–H₂O. *Am. Mineral., 58,* 277–286.

Thompson, J. B., Jr. (1955) The thermodynamic basis for the mineral facies concept. *Am. J. Sci., 253,* 65–103.

Tuttle, O. F. (1949) Two pressure vessels for silicate–water studies. *Geol. Soc. Am. Bull., 60,* 1727–1729.

Veblen, D. R. and C. W. Burnham (1975) Triple-chain biopyriboles: newly discovered intermediate products of the retrograde anthophyllite-talc transformation, Chester, Vt. (abstr.). *Trans. Am. Geophys. Union, 56,* 1076.

—— and —— (1976) Biopyriboles from Chester, Vermont: the first mixed-chain silicates (abstr.). *Geol. Soc. Am. Abstracts with Programs, 8,* 1153.

——, P. R. Buseck and C. W. Burnham (1977) Asbestiform chain silicates: new minerals and structural groups. *Science, 198,* 359–365.

Zen, E-an (1969) Free energy of formation of pyrophyllite from hydrothermal data: values, discrepancies and implications. *Am. Mineral., 54,* 1592–1606.

—— (1971) Comments on the thermodynamic constants and hydrothermal stability relations of anthophyllite. *Am. J. Sci., 270,* 136–150.

—— (1972) Gibbs free energy, enthalpy and entropy of ten rock-forming minerals: calculations, discrepancies, implications. *Am. Mineral., 57,* 524–553.

—— and J. V. Chernosky, Jr. (1976) Correlated free energy values of anthophyllite, brucite, clinochrysotile, enstatite, forsterite, quartz and talc. *Am. Mineral., 61,* 1156–1166.